FEM-BASED CONFINEMENT MODEL FOR AXIALLY LOADED COLUMNS RETROFITTED BY PRESTRESSED ARAMID FIBER BELTS

Kooroush NASROLLAHZADEH NESHELI [*1] and Tetsuo YAMAKAWA[*2]

ABSTRACT: An analytical model based on nonlinear 3-D finite element method is introduced in this paper to consider the active and passive confinement provided by prestressed aramid fiber belts. The model is also applied to concrete columns wrapped with FRP sheets, and is verified by experimental results reported for axially loaded concrete columns retrofitted by AFRP sheets. The model is able to account for the influence of different corner radii of square sections on stress-strain curve. Finally, through a parametric study, it is shown that providing active confinement can save the consumption of new materials, while the stress-strain curves are similar to those for only passive confinement provided by AFRP sheets but with thicker plies.
KEYWORDS: RC column, passive confinement, active confinement, prestressed aramid fiber belt, strain, stress, finite element method

1. INTRODUCTION

Confinement of concrete is the key to mechanically enhance the strength and ductility of plain concrete. Two different sorts of confinement can be distinguished as follows: passive and active confinement. Passive confinement controls the lateral expansion of concrete and can be achieved, for instance, by casting concrete in steel or fiber reinforced polymer (FRP) tubes, or by wrapping the concrete with steel plate or FRP sheets. When the concrete is axially loaded, lateral expansion is then restrained by the confining device, resulting in lateral pressure at the interface. As the axial load increases, the tendency for lateral expansion increases and therefore the confining pressure increases. The amount of confining pressure is the function of dilation characteristics of concrete, which in turn, depend on the lateral stiffness of the confining device. On the other hand, active confinement, which can be achieved by prestressing the confinement material before applying axial load to the concrete, is independent on the lateral expansion of concrete, and thereby, it is independent on the lateral stiffness of confining material.

One method to achieve active confinement as well as passive confinement is the confinement of concrete by use of prestressed aramid fiber belts. The past experimental studies have shown the high efficiency of the proposed technique to develop a ductile flexural response for the columns which basically failed in a shear manner because of their poor transverse steel reinforcement [1]. This paper proposes an analytical model based on nonlinear 3-D finite element method to establish stress-strain curves for concrete confined by prestressed aramid fiber belts.

2. RETROFIT BY PRESTRESSED ARAMID FIBER BELTS

Fig. 1 shows the details of retrofit technique. In this technique, aramid fiber belt is cut and impregnated with epoxy resin along only 100 mm lap joint of both cut ends to form a loop, which is straightened to form a two-ply belt. Both ends of the two-ply belt after being straightened look like eye-hook, through which crossbar can be put. It should be explained that crossbar refers to a piece of steel which has a threaded

*1 Graduate Student, Univ. of the Ryukyus, M.Sc., Member of JCI
*2 Prof., Department of Civil Eng. & Architecture, Univ. of the Ryukyus, Dr.E., Member of JCI

hole at its both ends. When the two-ply belt is wound around the column, its both ends can be clamped together by putting a couple of crossbars into the end eye-hooks, and then, passing bolt through the threaded hole of crossbar. The prestressing can be given to the belts by manually screw driving the bolts of crossbars. In **Fig. 1**, the assembly of a couple of crossbars and bolts is referred to as coupler. Steel angles, which are located at the corners of the column, have width and length of 50 mm and thickness of 20 mm. The role of steel angles is to protect corner concrete from the bearing failure. An external radius of 20 mm is provided for the corner angle in order to decrease stress concentration in the belt. Moreover, a frictionless film, which is placed between corner angle and belt, reduces the friction between belt and corner angle.

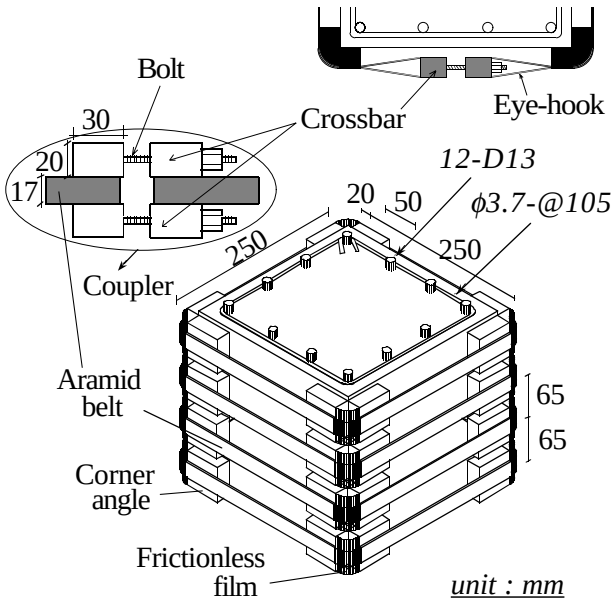

Fig. 1 Details of retrofit

3. FINITE ELEMENT MODELING

Knowing the constitutive laws of confined concrete is a fundamental study to predict the behavior of retrofitted RC columns. Analytical models for concrete confined by FRP materials must be able to account for the unique characteristics of concrete when confined with linear-elastic and non-yielding materials. In spite of steel tubes, where the confining pressure is constant after yielding the steel, the induced confinement provided by FRP materials is variable because of non-yielding properties of such materials. It is therefore clear why Mander's stress-strain curve [2], which is based on a constant confining pressure, can not be used to model the passive confinement of FRP materials. Instead, Mander's model is able to consider active confinement, where the confinement is neither variable nor dependent on the axial load level. On the other hand, previous researchers have definitely shown the influence of corner radius on stress-strain curve of square sections confined by FRP materials [3]. Therefore, in order to propose an analytical model for square sections, attention should be paid to the corner radius of cross section.

Considering the above-mentioned requirements, a FEM-based model by use of Micro-DIANA is proposed in this paper. Although the declared objective of this paper (as appeared in the title) is prestressed aramid fiber belt, in order to verify the proposed approach with experimental results reported by Masuo et al. [3], the model is also applied to AFRP sheet. The column retrofitted by aramid fiber belt is 250 mm square section (see **Fig. 1**), while the column confined with AFRP sheet is 300 mm square section. **Figs. 2** and **3** show FEM meshes for AFRP sheet and aramid fiber belt, respectively. Both of meshes consider one quarter of cross section due to symmetry. The confining material is modeled by use of nonlinear translation springs. For the case of AFRP sheets, the springs are distributed on the perimeter of cross section, while in the case of aramid fiber belts the springs are considered only at the corners, because the belts are supported on the corner angles and there is a clear space (20 mm) between the belts and column surface in the other parts of cross section (see **Fig. 1**). The model of AFRP sheet takes into account different corner radii of cross section (R= 10, 30 mm). In case of aramid fiber belt, the external radius of corner angle is considered as corner radius of cross section, that is R= 20 mm (see **Fig. 1**). Therefore, steel angle has not been modeled in the mesh. This is because steel angle is for transmitting the confining force from belt to concrete and distributing the stresses in the concrete near the corners, and thus, its influence is local and for simplicity of model, it can be ignored when the general behavior of concrete, such as stress-strain relationship, needs to be modeled. **Table 1** shows properties of materials. One layer mesh with thickness of 10 mm is loaded by uniform axial displacement applying at the top of the mesh. Therefore, the analysis is based on displacement control by gradually increasing the axial compression displacement.

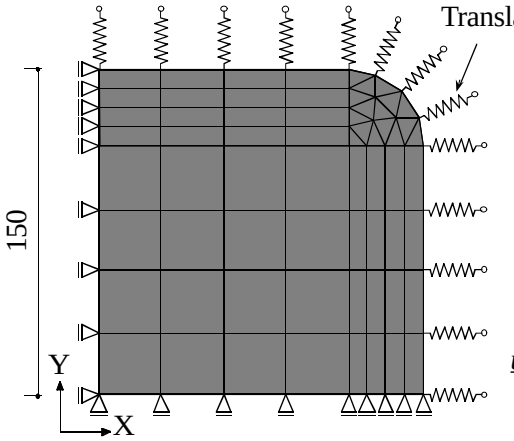

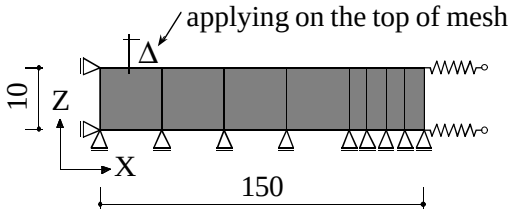

Fig. 2 FEM mesh for AFRP sheet

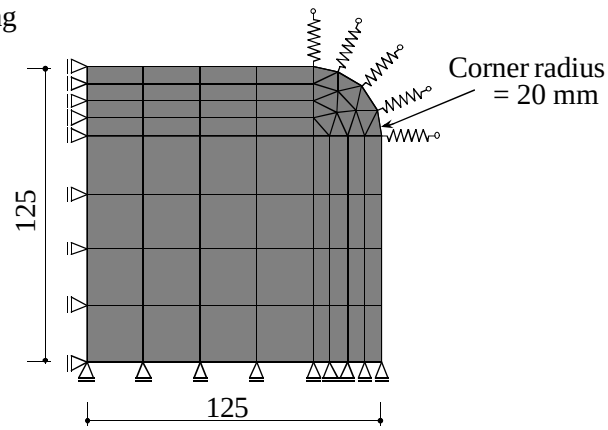

Fig. 3 FEM mesh for aramid fiber belt

Table 1 Properties of materials

Type	f_y (MPa)	ε_y (%)	E (GPa)
Aramid fiber belt/AFRP sheet	2065	1.75	118

Notes: f_y and ε_y = design strength and strain, E = Young modulus; AFRP sheet is 4-ply (each ply is 0.43 mm thick), Aramid fiber belt is 2-ply @ 65 mm (each ply has width of 17 mm, thickness of 0.612 mm, cross section area of 10.4 mm^2).

In the FEM model, the concrete is modeled with three-dimensional solid elements. To analyze passive confinement, the input constitutive law for concrete is considered as **Fig. 4**. Mander's formula is used to model behavior of plain concrete in compression. The confinement effect is then automatically considered by the surrounding springs through the analysis. However, to consider active confinement, the input compression behavior for concrete is different and will be explained later. The concrete cylindrical strength (σ_B) for the columns confined with AFRP sheet is 29.4 MPa [3], while σ_B for columns retrofitted by aramid fiber belts is 23.4 MPa [1]. In the tension zone of concrete, a crack arises if the major principal tensile stress exceeds the tensile strength (σ_{cr}). Smeared cracking and linear tension softening is adopted in the model. Shear retention, that is reduction in the shear stiffness due to the cracking of the material, is generally dependent on the crack width. To take into account this phenomenon, a variable shear retention factor, which is a function of the normal crack strain is considered in this paper, according to the following equation:

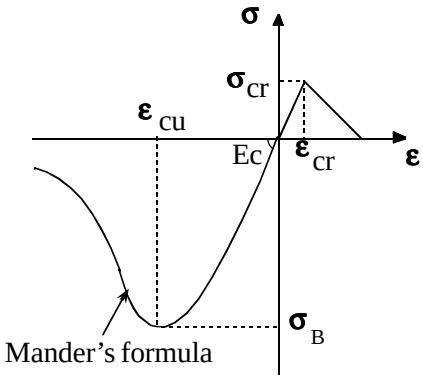

Fig. 4 Unconfined concrete

$$\beta = \frac{1}{1 + 4447\,\varepsilon_n} \qquad (1)$$

where, β is shear retention factor and ε_n is normal crack strain.

Drucker-Prager is used for the plasticity-based model of concrete. The yield condition is given by:

$$f(I_1, J_2) = \alpha I_1 + \sqrt{J_2} - k = 0 \qquad (2)$$

$$\alpha = \frac{2\sin\phi}{\sqrt{3}\,(3-\sin\phi)} \qquad (3)$$

$$k = \frac{6\cos\phi}{\sqrt{3}\,(3-\sin\phi)}\,c \qquad (4)$$

$$I_1 = \sigma_1 + \sigma_2 + \sigma_3 \quad (5)$$

$$J_2 = [\ (\sigma_1 - \sigma_2)^2 + (\sigma_2 - \sigma_3)^2 + (\sigma_3 - \sigma_1)^2\ ] / 6 \quad (6)$$

In Eqs. 3 and 4, ϕ is the angle of internal friction and c is the cohesion. In Eqs. 5 and 6, σ_1, σ_2 and σ_3 are the principal stresses. In this paper, the associated flow rule is used. Although the internal friction angle is taken as equal to the dilatancy angle, the proposed FEM model deals with dilation characteristics of concrete not only through the introduced flow rule but also, and more importantly, through the inserted surrounding translation springs which provide lateral stiffness against dilation of concrete. The important parameter of Drucker-Prager is the internal friction angle that must be determined based on experimental results appropriate to the purpose of analysis. Herein, to describe the behavior of concrete in a triaxial state of stress with variable confining pressure, Richart's formula [4] is adopted. According to Richart's formula, which is based on large experimental database and has been widely used by many researchers for confinement of concrete, the strength of concrete confined by a lateral pressure (σ) increases to ($\sigma_B + 4.1\ \sigma$), where σ_B is the cylindrical strength of concrete. From this formula, a set of principal stresses which corresponds to the yield condition is recognized, that is: $\sigma_1 = \sigma_2 = -\sigma$, $\sigma_3 = -(\sigma_B + 4.1\ \sigma)$. The minus refers to compression. By substituting this state of principal stresses into yield condition (Eq. 2), we reach :

$$(1- \alpha\sqrt{3}\ )\ \sigma_B + (3.1- 6.1\ \alpha\sqrt{3}\ )\ \sigma - k\sqrt{3}\ = 0 \quad (7)$$

Moreover, because Richart's formula proposes a constant coefficient of 4.1 for any value of confining pressure; therefore, the Eq. 7 must be valid for any confining pressure σ , as well. And considering that friction angle, and thereby α , are constant values; satisfaction of Eq. 7 requires that the multiplication factor of second term in Eq. 7 must be zero:

$$(3.1- 6.1\ \alpha\sqrt{3}\ ) = 0 \quad \Rightarrow \quad \phi = 37.5^\circ \quad (8)$$

This value of ϕ ensures that under any confining pressure, Eq. 7 is satisfied. Therefore, the friction angle of 37.5 degrees is most likely to be appropriate to the case of triaxial state of stress with respect to Richart's formula. By adopting this value for ϕ, the remained terms of Eq. 7 give $c = 0.246\ \sigma_B$, which describes the cohesion as proportional to the concrete cylindrical strength by the coefficient of 0.246 that is suitable for triaxial state. Another aspect of the model is the stiffness values of the translation springs. Herein, experimental data by Masuo et al. [3], which are for AFRP sheets (note that for prestressed aramid fiber belts, experimental data on stress-strain curve have not yet been reported), are employed to calibrate the stiffness of springs. Using a trial and error approach, the stiffness of the springs in case of AFRP sheet

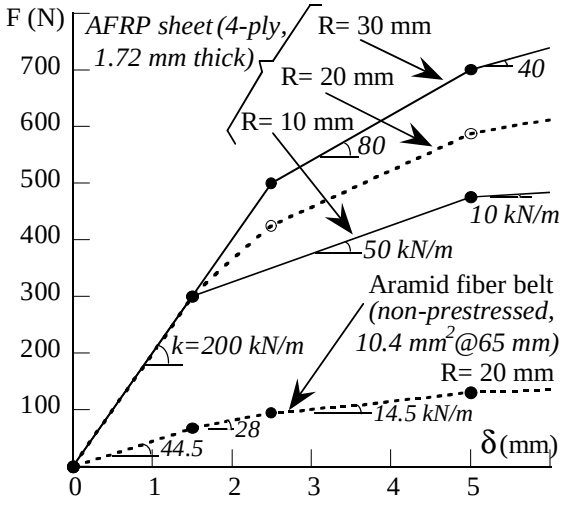

Fig. 5 Force-Displacement (F-δ) curves for springs

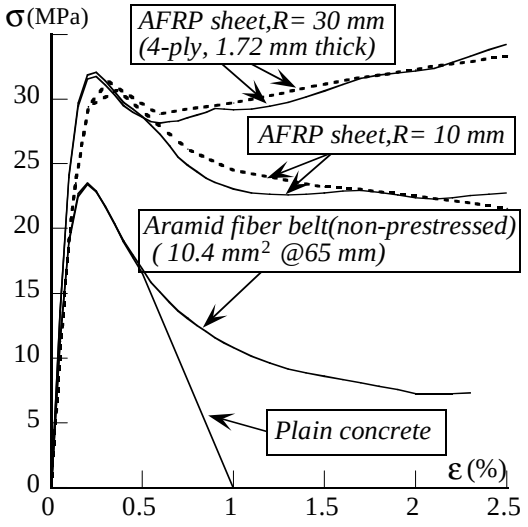

Fig. 6 Calculated and experimental stress-strain

(see **Fig. 2**) is iteratively modified in order that the analytically resulted stress-strain curve can be matched with the reported experimental stress-strain relationship [3]. The solid lines in **Fig. 5** show the suggested diagrams for the force-displacement relationships of the springs in the case of AFRP sheets with two different corner radii of R= 10 and 30 mm. In **Fig. 5**, the values of spring stiffness *k*, that is the slope of force-displacement diagram, are also shown. **Fig. 6** compares the analytical results for AFRP sheet (R= 10 and 30 mm) with the experimental results reported by Masuo et al. [3]. As it can be seen, the suggested curve for force-displacement, which is nonlinear, can give a good agreement with the experiments.

Although a trial and error scheme was used to derive the stiffness of springs in case of AFRP sheets, the stiffness values for prestressed aramid fiber belts (see **Fig. 3**) can be directly concluded from those derived for AFRP sheets, based on some assumptions, as follows. The stiffness of springs is related to the lateral stiffness of confining material which is linearly proportional to (EA / l), where E and A are elasticity modulus and cross section area of confining material respectively, and l is the lateral length of confining device that is equal to depth of concrete section. Considering that AFRP sheet is 4-ply (each ply is 0.43 mm thick) and depth of the column is 300 mm (see **Fig. 2**), but aramid fiber belt is 2-ply (each ply is 10.4 mm^2 in area) located at the intervals of 65 mm (see **Fig. 1**) with the column depth of 250 mm, therefore the spring stiffness for aramid fiber belt is calculated to be equal to 0.22 times the spring stiffness in case of AFRP sheet. And, to have spring stiffness for the corner radius of R= 20 mm (as suitable for aramid fiber belt), the average of proposed stiffnesses for R= 10 mm and for R= 30 mm is considered. **Fig. 5** shows the assumed force-displacement curve for aramid fiber belts, and **Fig. 6** presents the corresponding calculated stress-stain curve for confinement by aramid fiber belts.

4. CONSIDERATION OF ACTIVE CONFINEMENT

As explained earlier, Mander's stress-strain curve [2], which is based on a constant confining pressure, can be used to model the active confinement. The peak confined strength σ_{BC} is a function of the unconfined strength σ_B and the constant lateral confining pressure σ_R as follows:

$$\sigma_{BC} = \sigma_B \left[2.254\sqrt{1 + \frac{7.94\,\sigma_R}{\sigma_B}} - 2\frac{\sigma_R}{\sigma_B} - 1.254 \right] \quad (9)$$

$$\sigma_R = k_e \cdot \frac{2\sigma_p A_a}{b\,s} \quad , \quad k_e = \left(1 - \sum_{i=1}^{n} \frac{(w'_i)^2}{6\,b^2}\right)\left(1 - \frac{s'}{2b}\right)^2 \quad (10)$$

The k_e is confinement effectiveness coefficient, that is the ratio of effectively confined area to the total cross section, and it can be calculated by assuming the arching action to act in the form of second-degree parabolas with an initial tangent slope of 45° (see **Fig. 7**). The σ_p is the prestressing stress, A_a is the cross section area of 2-ply belt, and s is the interval of belts. In this case, k_e is equal to 0.72 (n= 4, s'= 15 mm, w'$_i$ = 150 mm). For the aramid fiber belts (2-ply @65 mm) with prestressing levels of one-third and one-half of design strength of aramid fiber material (see **Table 1**), the effective confining pressures σ_R are 1.26 and 1.89 MPa, respectively. Considering these values for σ_R in Eq. 9 and using Mander's model, the stress-strain curves for only active confinement are calculated as shown in **Fig. 8**. These calculated stress-strain relationships are considered as constitutive laws of concrete in compression and input in the FEM model (as replacement of **Fig. 4**).

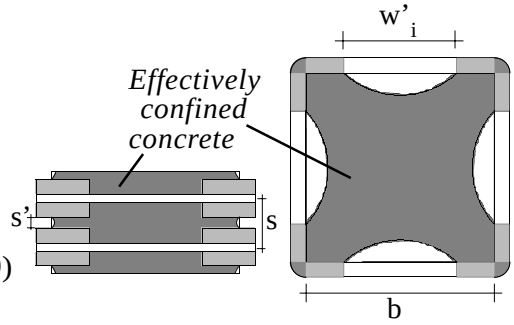

Fig. 7 Effectively confined concrete

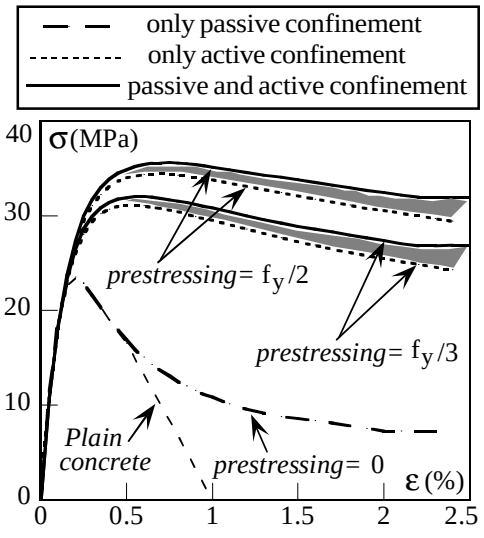

Fig. 8 Calculated stress-strain curves of confinement by aramid fiber belt

Therefore, the active confinement is taken into account by directly applying Mander's formula, and passive confinement is considered by nonlinear springs. The results of analysis (active and passive confinement) are shown in **Fig. 8**. The hatched areas in **Fig. 8**, show the effect of passive confinement on the total behavior of confined concrete. The passive effect is small because of small amount of consumed materials for the aramid fiber belts, that leads to more important role of active confinement in improving the stress-strain behavior of concrete confined by prestressed aramid fiber belts.

5. PARAMETRIC STUDY

The study is extended to compare stress-strain curves for different number of plies of AFRP sheet with those for prestressed aramid fiber belts. **Fig. 9** shows the calculated results for two corner radii of R= 10 and 30 mm. It should be noticed that the result for aramid fiber belt, which is mainly governed by active confinement, is less influenced by the corner radius. But, corner radius has considerable influence for AFRP sheet, especially when the number of plies increases. The volume of consumed material for aramid fiber belt (@65 mm) is equal to that of an AFRP sheet with thickness of 0.3 mm, that is equal to 0.7-ply of sheet. It can be seen from **Fig. 9** that aramid fiber belt with prestressing of fy/3 behaves similar to AFRP sheet (R=10 mm) with 6-ply; while the consumed material is much less than that of sheet. This fact endorses the efficiency of prestressing to save the material. The results of AFRP sheet for greater value of corner radius R=30 mm, show an almost bilinear stress-strain curve with an ascending branch (see **Fig. 9**). This sort of stress-strain is similar to that of circular sections confined by FRP material, as reported by early investigators. Therefore, it is expected that increasing the corner radius of square sections can develop better passive confinement for AFRP sheets.

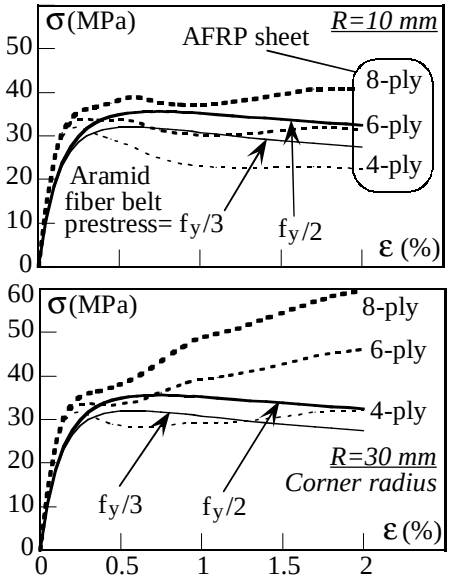

Fig. 9 Calculated stress-strain curves for AFRP sheet and aramid fiber belt

6. CONCLUSIONS

In this paper by use of nonlinear 3-D finite element method and in order to predict stress-strain curves for square sections, it has been shown that passive confinement provided by AFRP sheets or prestressed aramid fiber belts can be interpreted as nonlinear translation springs. Drucker-Prager criterion with the internal friction angle $\phi = 37.5^\circ$ and associated flow rule is adopted in the FEM model. In square sections, the more corner radius can provide more lateral stiffness for confining device, and thereby can develop better passive confinement. The active confinement is considered by introducing the concrete constitutive law calculated by Mander's formula for constant confining pressure into the FEM model.

REFERENCES

1. Yamakawa, T., Nasrollahzadeh Nesheli, K. and Satoh, H., "Seismic or Emergency Retrofit of RC Short Columns by use of Prestressed Aramid Fiber Belts as External Hoops," J. of Structural and Construction Engineering (Transactions of AIJ), No. 550, Dec. 2001, pp.135-141.
2. Mander, J. B., Priestley, M. J. N. and Park, R., "Theoretical Stress-Strain Model for Confined Concrete," J. of Structural Engineering, ASCE, Vol. 114, No. 8, Aug. 1988, pp.1804-1826.
3. Sugimoto, T., Masuo, K., Tanigaki, M. and Sumida, A., "The Effect of AFRP and CFRP Sheet Jacketing on the Compressive Behavior of Reinforced Concrete Columns," Proc. of Japan Concrete Institute, JCI, Vol. 21, No. 3, 1999, pp.1489-1494. (in Japanese)
4. Richart, F. E. et al., "A Study of the Failure of Concrete under Combined Compressive Stresses," University of Illinois, Engineering Experimental Station, Bulletin No. 185, Univ. of Illinois, 1928.11.